11.B.1

Land Surface Modeling in the Navy Operational Global Atmospheric Prediction System

Timothy F. Hogan
Naval Research Laboratory
Monterey, CA 93943

1. INTRODUCTION

The Navy Operational Global Atmospheric Prediction System (NOGAPS) is the U. S. Department of Defense (DoD) high-resolution (T239L30) global weather prediction system. Its development and operation is a joint activity of the Naval Research Laboratory (NRL) and the U.S. Navy's Fleet Numerical Meteorology and Oceanography Center (FNMOC). NOGAPS forecasts provide high-resolution 7.5 day forecasts every six hours and a daily-extended 10 day guidance using the FNMOC ensemble (T119L30), to numerous defense and civilian users. NOGAPS products are used as boundary conditions and forcing for a large number of DoD environmental and application systems. Prominent among these applications are the U.S. Navy's Coupled Ocean-Atmosphere Mesoscale Prediction System, FNMOC's version of NOAA's Geophysical Fluid Dynamics Lab tropical cyclone model, which is called GFDN, the U.S. Navy's Aerosol Analysis and Prediction System (NAAPS), and the calculation of the effective atmospheric angular momentum functions (Barnes, et al. 1983) for the Naval Observatory's precise time keeping program. NOGAPS is also used as the principal tool in the U.S. Navy's extensive global numerical weather prediction (NWP) research programs.

Recent changes to NOGAPS include the introduction of new land surface modeling (LSM) schemes, developed by the Naval Research Laboratory. The new LSM schemes replaced the simple single layer slab/bucket scheme. Data assimilation results for July 2006 demonstrated that the introduction of the LSM schemes reduced NOGAPS land surface cold bias and improved the prediction of tropical cyclone track forecasts. The current presentation will include: (1) the current formulation of the NOGAPS LSM scheme (version 1) , (2) summer and winter NOGAPS data assimilation results with the new LSM schemes vs. NOGAPS with a slab land modeling scheme, (3) sensitivity experiments of some of the snow parameters in the LSM, and (4) planned improvements of the NOGAPS LSM scheme.

2. CURRENT NOGAPS LSM

There are 3 distinct modules for the LSM schemes in NOGAPS: (1) a module that computes the fluxes and surface land temperature, (2) a module for the calculation of the surface albedo, and (3) a module for the calculation of the sub-soil temperature, liquid water, and ice water content. Each module is a separate and independent subroutine package, enabling the flux calculations to be tied directly to the PBL calculations, the albedo calculations to be performed immediately before the radiation calculations, and the sub-soil temperature and water calculations immediately after the rain-fall parameterizations.

In the flux and surface module a composite surface temperature equation is solved, which is given by

$$c_s \frac{dT_s}{dt} = F_{SW} + F_{LW} - \sigma T_s^{\,4} - LE - SH \,. \qquad (1)$$

This equation is solved by coupling it directly to the PBL subroutine and implicitly solving together the surface and air temperatures through a tri-diagonal solver. In equation (1) T_s is the composite soil/vegetation temperature, c_s is the composite surface heat capacity, F_{SW} is the total solar radiation, F_{LW} is the downward long-wave radiation, σ is the Stefan-Boltzmann constant, LE is the latent heat cooling, and SH is the sensible heat release. The composite surface heat capacity is given by

$$c_s = a_{veg} c_{veg} + (1 - a_{veg}) c_{soil} \,, \qquad (2)$$

where a_{veg} is the fractional that is covered by vegetation, c_{veg} is a type dependent vegetation heat capacity, and c_{soil} is the type dependent soil heat capacity. Similarly, the latent and sensible heat releases are computed as

$$LE = a_{veg} LE_{veg} + (1 - a_{veg}) LE_{soil} \qquad (3)$$

and

$$SH = a_{veg} SH_{veg} + (1 - a_{veg}) SH_{soil} \,. \qquad (4)$$

The soil portions of the latent and sensible heat are computed using the Louis (1979) surface flux formulation. The vegetation portion of the latent heat is restricted to evapotranspiration release as given by Wetzel and Chang (1988). An additional limit is set on evapotranspiration to prevent excessive drying out of the soil. There are 23 different vegetation types and 13 different soil types, which are specified as the dominate vegetation and soil type in a box centered at the computational grid. The data bases are from U.S.D.A. and FAO vegetation and soil data bases. The vegetation a_{veg} fraction is determined from a 5-year climatology data set (Gutman and Ignatov, 1998). If snow is present with sufficient depth (1 cm) the surface is assumed to be uniformly covered with snow with no vegetation effects and the snow heat capacity is used for c_s.

The surface albedo is computed in a similar manner as latent and sensible heat, namely

$$\alpha_s = a_{veg}\alpha_{veg} + (1 - a_{veg})\alpha_{soil} . \qquad (5)$$

The vegetation albedo is type dependent, ranging between 0.07 – 0.15. The soil albedo depends on soil color (light, medium, or dark) and soil-wetness GW. For light colored soils:

$$\alpha_{soil} = 0.18 + 0.25(1 - GW) , \qquad (6a)$$

for medium color soils:

$$\alpha_{soil} = 0.10 + 0.20(1 - GW) , \qquad (6b)$$

and for dark soils:

$$\alpha_{soil} = 0.07 + 0.15(1 - GW) . \qquad (6c)$$

If snow is present at sufficient depth, the albedo is set to 0.84, except for tree covered areas, where a limit is set of 0.15 to the maximum albedo. This will be discussed in Section 4.

The soil model consists of 4 layers down to a depth of 2 meters. Standard diffusion-type predictive equations are solved for the soil temperatures and soil moisture. The soil parameters for the soil moisture movement are taken from Clapp and Hornberger (1978). Rain and melting snow are allowed into the top soil level until saturation occurs. If the soil temperature falls above/below freezing, the soil liquid water is converted to soil water/ice. The top soil temperature is taken to be T_s, which is provided from the PBL calculations (Eq. 1). If snow is present, the snow depth is treated as an extra level. A boundary condition of deep soil temperature climatology is used, which was computed from output from the US Air Force AGRMET system.

3. DATA ASSIMILATION AND MEDIUM RANGE FORECAST RESULTS

In order to ascertain the impact of the new LSM data assimilation and medium range forecast tests were conducted with the new LSM schemes. The data assimilation was performed with U.S. Navy's 3-dimensional data assimilation system NAVDAS (Navy Atmospheric Variational Data Assimilation System) (Daley and Barker 2001), coupled to the forecast model NOGAPS. The results of the tests were contrasted with the results of the operational system, with the single layer slab model. The periods of the tests are July 2006 (a summer case) and January 2006 (a winter case).

Figs. 1-3 are the 500-mb anomaly correlations (AC) with the new LSM schemes (labeled LSM1) vs. the corresponding AC for the operational forecasts (labeled OPS) for July 2006. Over the Southern Hemisphere (Fig. 1) the forecast skill is neutral when compared to the operational results, but in the Northern Mid-latitudes the forecast skill is moderately improved throughout the 120 hr forecasts. In the Arctic region (Fig. 3) there does appear a slight loss of skill at 60 - 96 h. Over all regions the lower level temperatures are warmer, either removing the cold bias seen in the slab version of NOGAPS or greatly reducing the bias. Fig. 4 shows the 1000-mb mean temperature error over North America for the July 2006 test period.

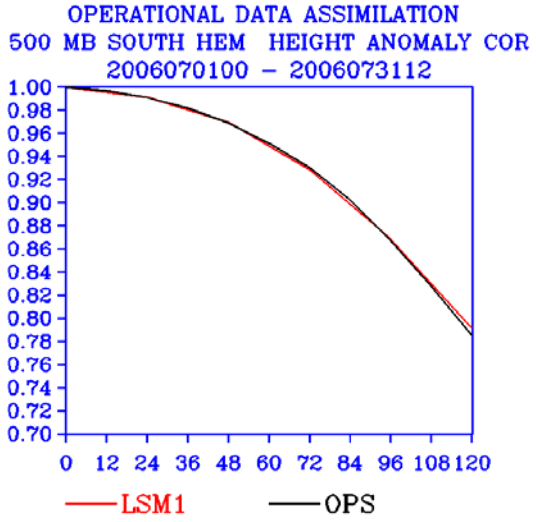

FIG. 1. A comparison of LSM1 and OPS 500-mb time-mean anomaly correlations vs. forecast hour for the Southern Hemisphere (20S – 80S) for the period of July 2006.

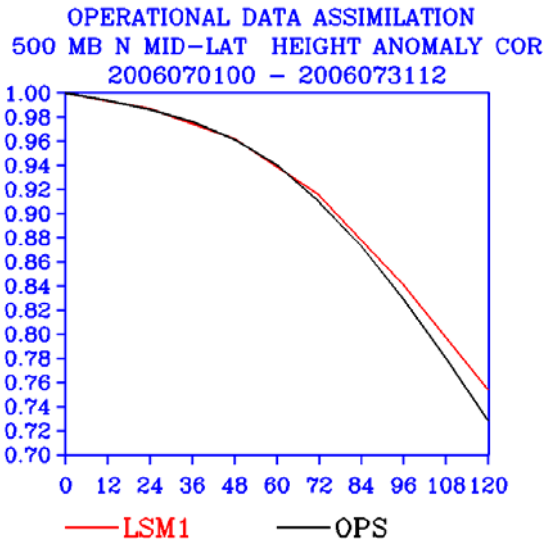

FIG. 2. A comparison of LSM1 and OPS 500-mb time-mean anomaly correlations vs. forecast hour for the Northern Mid-Latitudes (20N-60N) for the period of July 2006.

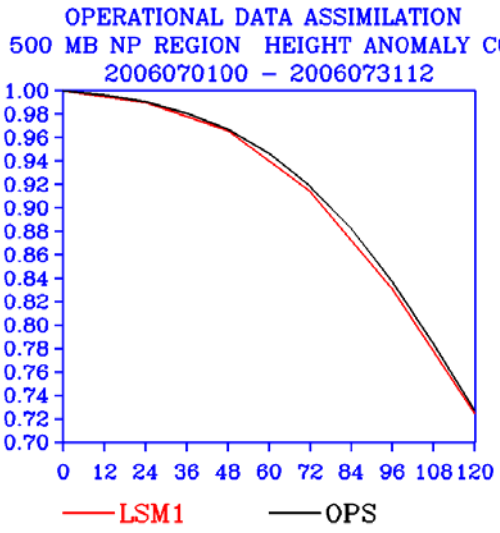

FIG. 3. A comparison of LSM1 and OPS 500-mb time-mean anomaly correlations vs. forecast hour for the Northern Polar Region (60N – 90N) for the period of July 2006.

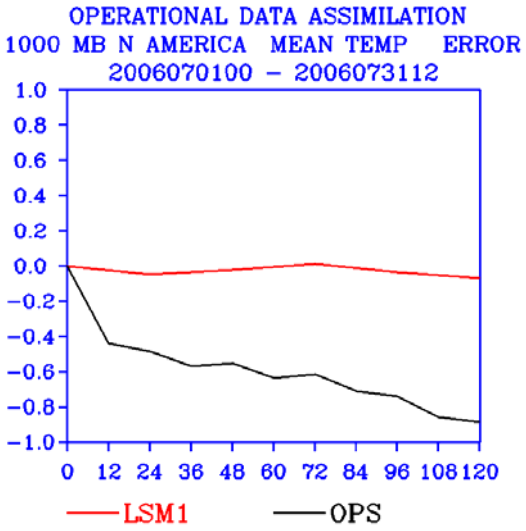

FIG. 4. A comparison of LSM1 and OPS 1000-mb time mean temperature bias over North America for the period of July 2006.

In addition to warmer surface temperatures observed in the Topics, there is a noticeable improvement in NOGAPS tropical cyclone (TC) tracks. Fig. 5 shows the TC results for the July 2006 tests. With the new LSM the TC results are improved by nearly 25-nm at 120-h, which represents a 12-h improvement in the TC track forecasts for NOGAPS.

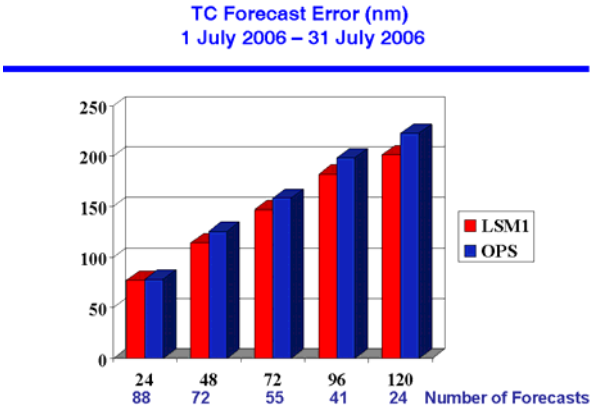

FIG. 5. A bar chart showing the comparison of the TC tracks errors in nautical mile for the new LSM schemes and the operational model of July 2006, which used the land slab model. The number of forecast tracks, which were used as verification at each forecast time, is listed below the forecast hour.

Figs 6-8 are the AC results for the different regions for the January 2006 forecasts. Each region shows a slight increase of forecast skill as measured by the AC score. As in the summer results, most land

regions demonstrate a warmer forecast at the surface, however the region north of 60N did show a notable cold bias as opposed to the warm bias using the slab land model (Fig 9).

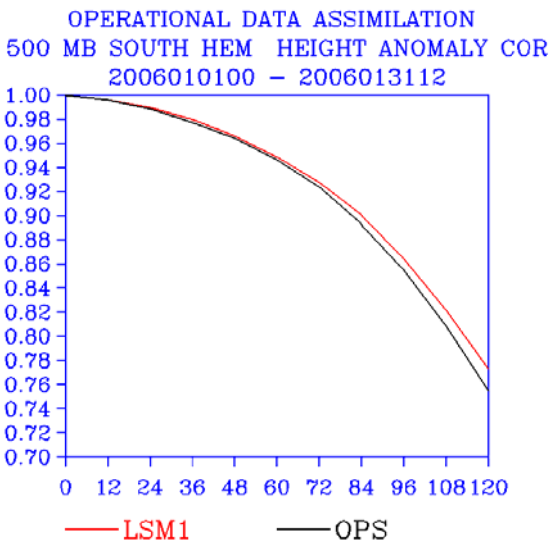

FIG. 6. A comparison of LSM1 and OPS 500-mb time-mean anomaly vs. forecast hour correlations for the Southern Hemisphere (20S – 80S) for the period of January 2006.

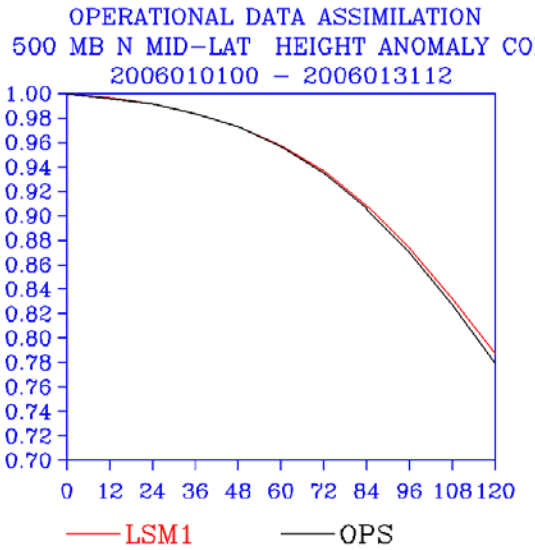

FIG. 7. A comparison of LSM1 and OPS 500-mb time-mean anomaly correlations vs. forecast hour for the Northern Mid-Latitudes (20N-60N) for the period of January 2006.

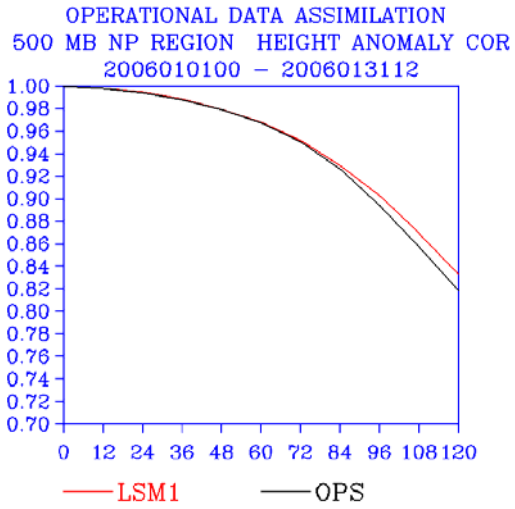

FIG. 8. A comparison of LSM1 and OPS 500-mb time-mean anomaly correlations vs. forecast hour for the Northern Polar Region (60N – 90N) for the period of January 2006.

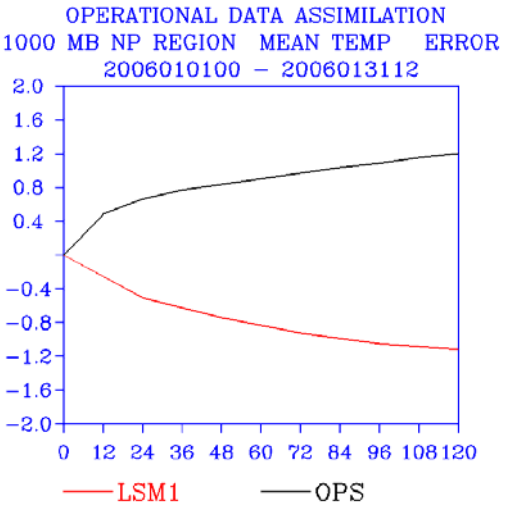

FIG. 9. A comparison of LSM1 and OPS 1000-mb time mean temperature bias over the Arctic region (60N-90N) for the period of January 2006.

4. SENSITIVITY RESULTS OF SOME OF THE SNOW PARAMETERS IN THE LSM.

The original transition of the LSM codes to operational NOGAPS occurred in August 2007. Testing proceeded on trying to improve the scheme, with particular emphasis on improving the surface temperature north of 60N. The original values of the snow thermal heat capacity h_{snow} and snow thermal

conductivity t_{snow} were set to values that are characteristic of new snow:

$$h_{snow} = 1.9256 \times 10^5 \, JK^{-1}m^{-3},$$

and

$$t_{snow} = 0.160 \, WK^{-1}m^{-1}.$$

Testing of larger values of h_{snow} and t_{snow} had a positive impact on reducing the cold bias. Fig. 9 shows a comparison of the 1000-mb temperature bias of the operational run (OPS) using the values of the snow parameters given above and a parallel beta-run (NEWSNP) revised (higher) values given by

$$h_{snow} = 5.7768 \times 10^5 \, JK^{-1}m^{-3}$$

and

$$t_{snow} = 0.480 \, WK^{-1}m^{-1}.$$

The RMS temperature error was also reduced by 1 degree (not shown). These values were subsequently transitioned to the operational code.

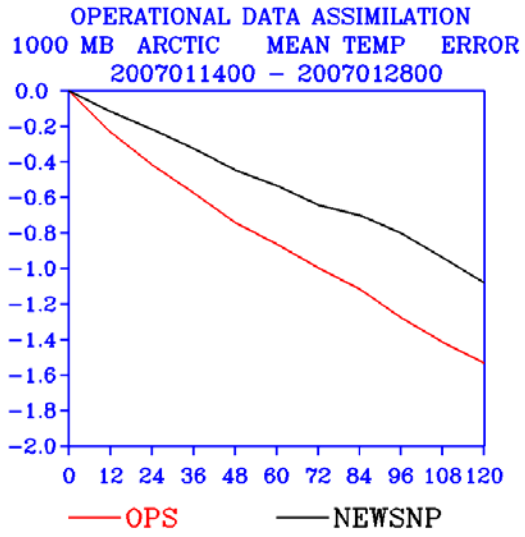

FIG. 10. A comparison of the 1000-mb mean temperature error for the OPS run and a parallel run with increased snow thermodynamic parameters over the Arctic region (60N-90N) for a 2-week period of January 2007.

A cold surface air temperature bias was also observed over the northern regions during the early spring of 2007. This was particularly dominant over the northern forested regions. Tests indicated that a limit set on the albedo of 0.15, which is similar to that used by ECMWF (IFS Documentation CY28r1, 2004), reduced the cold bias (Fig. 11) and lead to a slight improvement in the overall score of NOGAPS.

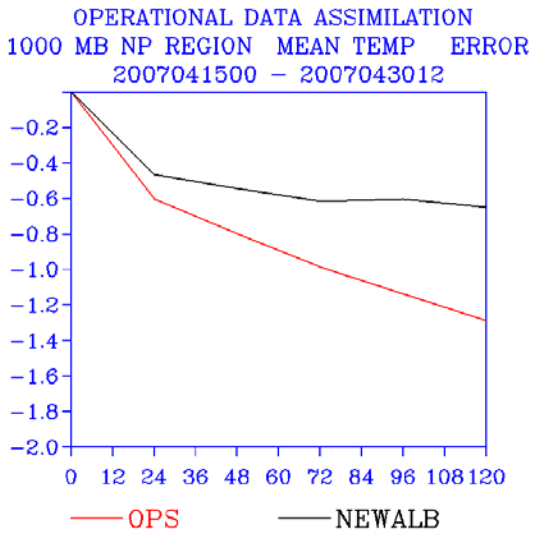

FIG. 11. A comparison of the 1000-mb mean temperature error for the OPS run and a parallel run with a limit set on the albedo for tall trees over the Arctic region (60N-90N) for a 2-week period of April 2007.

5. FUTURE PLANS

The transition of land surface schemes into NOGAPS marked a significant improvement in the NOGAPS forecasts of the lower level air temperatures. However, the simple scheme described here does not represent the state-of-the-science in LSM. Toward this end, new land surface parameterization schemes are under development that will include multiple tiles of vegetation, lake and urban schemes, ground temperature prediction beneath the vegetation, and snow properties based on snow-age.

Acknowledgements. The author gratefully acknowledges the support of Captain Michael Huff, METOC, IO, and ISR Program Manager (PMW-180), Project Number 0603207N.

REFERENCES

Barnes, R.T.H., R. Hide, A.A. White, and C.A. Wilson, 1983: Atmospheric angular momentum functions, length-of-day changes and polar motion. *Proc. R. Soc. Lond., A*, **387**, 31-73.

Clamp, R.B. and G.M. Hornbeger, 1978: Empirical equations for some soil hydraulic properties. *Water Resources Res*., **14**, 601-604.

Daley, R., and E. Barker, 2001: NAVDAS Source Book 2001: The NRL Atmospheric Variational Data

Assimilation System. NRL Publication. Available from NRL, Atmospheric Dynamics and Prediction Branch, Marine Meteorology Division, Monterey CA 93943-5502, 160 pp.

Gutman, G. and A. Ignatov, 1998: The derivation of the green vegetation fraction from NOAA/AVHRR data for use in numerical weather prediction models. *Int. J. Remote Sens*., **19(8)**, 1533-1543.

IFS Documentation CY28r1, 2004: http://www.ecmwf.int/research/ifsdocs /CY28r1/index.html

Louis, J. F., 1979: A parametric model of vertical eddy fluxes in the atmosphere. *Boundary Layer Meteorol.***, 17,** 187-202.

Wetzel, P.J and J.T. Chang 1988: Evapotranspiration from nonuniform surfaces: A first approach fro short-term numerical weather prediction, *Mon. Wea. Rev.* ,**116** 600-619.